

How to accurately measure the mobility and viscosity of two-dimensional carriers?

M.V. Cheremisin

A.F.Ioffe Physical-Technical Institute, St.Petersburg, Russia

(Dated: June 13, 2024)

Recently, a hydrodynamic behavior of ultrahigh mobility viscous two-dimensional electron gas in GaAs/AlGaAs quantum well was intensively studied based on relevant negative magnetoresistance (NMR) data. The two-dimensional Gurzhi model with(without) simplification combined with extra assumptions on electron-electron collisions rate often lead to a certain agreement with experiment. We provide ab initio analysis of the NMR data[Q. Shi et al, Phys. Rev. B. 89, 201301(R) (2014)] and demonstrate exceptional agreement with the uncut Gurzhi model attracting a single fitting parameter of the effective stream width. Our approach allows one to identify the intrinsic carrier mobility higher than that deduced by conventional methods. The NMR data analysis is proposed for powerful tool for two-dimensional viscometry.

PACS numbers:

I. INTRODUCTION

Starting from Gurzhi papers[1]-[3] the essential theoretical[4]-[9] and experimental efforts[10, 11] have been made to reveal hydrodynamic behavior of 2D electrons. The recent interest concerns the clean two-dimensional electron systems including high-mobility heterostructures, undoped graphene, and pure quasi-2D (semi)metals. The primary goal of the present paper is a study of electron fluid demonstrating giant NMR[12]-[26] and specific dependence of the resistance on the sample width[20],[26].

In general, it is adopted that the electron fluidity appears when the length of electron-electron interactions, l_{ee} , is less than typical sample size and, moreover, much less than the length, l_p , responsible for momentum transfer from electrons to lattice. For clarity, we further assume the elongated two-dimensional sample whose length l in x-direction is much greater than the width w . In presence of the perpendicular magnetic field $B = B_z$ the hydrodynamics approach implies that linearized Navier-Stokes equation

$$\frac{\partial \mathbf{V}}{\partial t} = \eta \Delta \mathbf{V} + [(\eta_H \Delta \mathbf{V} + \omega_c \mathbf{V}) \times \mathbf{e}_z] + \frac{e}{m} \mathbf{E} - \frac{\mathbf{V}}{\tau} \quad (1)$$

is valid for incompressible fluid when $\text{div} \mathbf{V} = 0$. Here, \mathbf{V} and \mathbf{E} are in-plane flux velocity and electric field respectively, ω_c is the cyclotron frequency, $\tau = l_p/v_F$ is the momentum relaxation time, v_F is the Fermi velocity. Then, $\eta = \frac{\eta_0}{\sqrt{1+(2l_{ee}/r_c)^2}}$ and $\eta_H = \frac{2l_{ee}}{r_c} \eta$ are the longitudinal and transverse(Hall) component[27] respectively of the viscosity tensor, $\eta_0 = v_F l_{ee}/4$ is the zero-field viscosity in two dimensions[9]. Finally, $r_c = v_F/\omega_c$ is the cyclotron radius.

Let us assume the electric field $E = E_x$ is applied along axis x . For steady state flow Eq.(1) yields the expression

$$\eta \frac{d^2 V}{dy^2} + \frac{e}{m} E_x - \frac{V}{\tau} = 0, \quad (2)$$

which provides the transverse profile of stream velocity $V(y)$. Similar to conventional 3D case[1] one may eas-

ily find[9] the average stream velocity and, in turn the resistivity

$$\rho = \rho_D \frac{1}{1 - \tanh(\xi)/\xi}. \quad (3)$$

Here, $\rho_D = \frac{mv_F}{ne^2 l_p}$ is the Drude resistivity, n is the 2D carriers density. Here, we introduce the dimensionless Gurzhi parameter $\xi = \xi_0 \sqrt{1 + (2l_{ee}/r_c)^2}$ whose zero-field value $\xi_0 = w/l_G$ is inversely proportional to specific Gurzhi length $l_G = \sqrt{l_{ee} l_p}$. Fortunately, a simple equation $\rho = \rho_D(1 + 3/\xi^2)$ provides excellent coincidence with Eq.(3) for both the low(high) limit $\xi \rightarrow 0(\infty)$ respectively. However, for intermediate range $\xi \sim 1$ the rough approach is shown[9] to give up to 10 percent error regarding the exact Eq.(3). In present study we will demonstrate the disadvantage of the approximative method which is, however, intensively explored in numerous studies[21–24].

Let us first consider the zero magnetic field case when $\xi = \xi_0$. Usually, the e-e interactions are much frequent compared to that owned to carriers scattering with phonons and(or) impurities, hence $l_{ee} < l_p$. For massive sample $\xi_0 \rightarrow \infty$ Eq.(3) reproduces the conventional Drude result, i.e. when $\rho = \rho_D$. By contrast, for ultra-clean low-size 2D system $\xi_0 \rightarrow 0$ the resistivity obeys the expression $\rho = \frac{m}{ne^2} \frac{3v_F l_{ee}}{w^2} \gg \rho_D$ resembling that known for Poiseuille flow in conventional hydrodynamics. We emphasize that the magnetic field enlarges the Gurzhi parameter $\xi > \xi_0$ depending on the ratio l_{ee}/r_c . Therefore, one expects that increase in magnetic field plays in favor to Drude transport scenario. This behavior is exactly that seen in experiment[17] reproduced in Fig.1a.

We now present self-consistent procedure which allows us to reproduce overall the resistivity set in Fig.1a. Recall again that the magnetic field destroys the hydrodynamic flow mode. Therefore, for each NMR curve in Fig.1a we find a unique point (ρ^*, B^*) whose flatness guarantees that the Drude regime has been achieved. The resulting dependence $\rho^*(B^*)$ is shown by squares in Fig.1a. Since each point of flatness corresponds to a certain

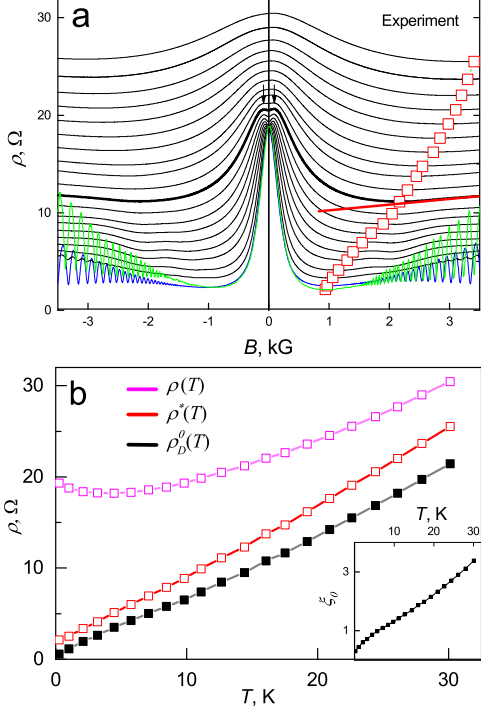


FIG. 1: a) Magneto-resistivity $\rho(B)$ at fixed temperature $T = 0.25\text{K}$ (green) $T = 1\text{K}$ (blue) and the temperature range $T = 2.1 - 30.1\text{K}$ (black) reproduced under Ref.[17]. Red marks depict the points of flatness (ρ^*, B^*) discussed in text. Bold curve and red line demonstrate the resistivity and its slope $\gamma = 0.57$ respectively at $T = 11.1\text{K}$. b) Temperature dependencies of the zero-field total $\rho(T)$, Drude $\rho_D^0(T)$ and resistivity owned to point of flatness $\rho^*(T)$. Inset: temperature dependence of the zero-field Gurzhi parameter $\xi_0(T)$.

temperature we plot the dependence $\rho^*(T)$ in Fig.2,b. To proceed, we underline that the all resistivity curves above points of flatness demonstrate a positive magneto-resistance, i.e. $\gamma = \frac{d\rho}{dB} > 0$. Our check of the data in Fig.1a gives a nearly constant slope $\gamma = 0.57\Omega/\text{kG}$ for all NMR curves. In view of the above finding the Drude resistivity entered in Eq.(3) must be modified as $\rho_D = \rho_D^0 + \gamma B$. Here, ρ_D^0 is the zero-field Drude resistivity. At fixed temperature and upon magnetic field enhancement the resistivity first drops within hydrodynamic regime and, then the increases because of Drude positive magneto-resistance. The respective minima can be attributed to experimental points of flatness discussed earlier. We argue that for actual mode $l_{ee}/r_c \gg 1$ of viscosity suppression the dimensionless Gurzhi parameter yields $\xi \sim 2\xi_0 l_{ee}/r_c = aB$. Consequently, Eq.(3) can be simplified as it follows

$$\rho = (\rho_D^0 + \gamma B)(1 + 1/aB), \quad (4)$$

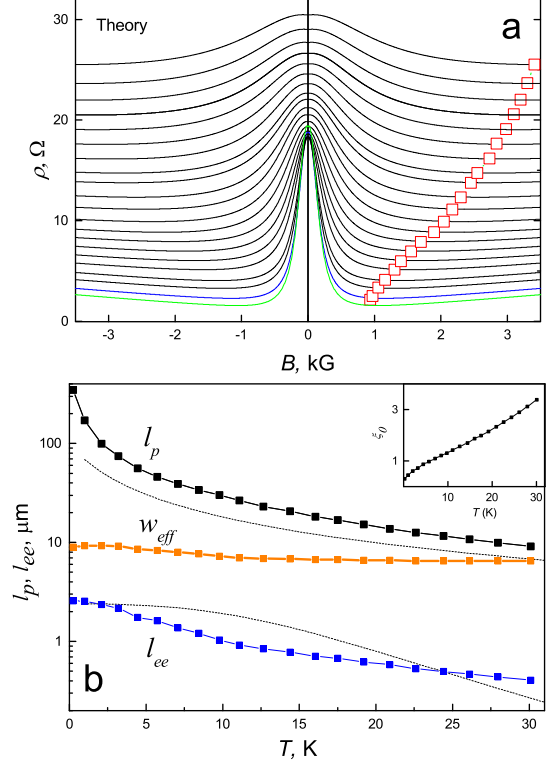


FIG. 2: a. The result of calculations provided the best fit of the resistivity data in Fig.1a. b. The scattering lengths $l_{ee}(T), l_p(T)$ and the effective width $w_{eff}(T)$ extracted from experimental data in Fig.1a. Dotted lines depict the result of Ref.[9].

whose primitive analysis gives the magnetic field $B^* = \sqrt{\frac{\rho_D^0}{a\gamma}}$ at the minima. Substituting the above value into Eq.(4) we find out the relationship

$$\rho_D^0 = \frac{\rho^*}{2} - \gamma B^* + \sqrt{\left(\frac{\rho^*}{2}\right)^2 - \rho^* \gamma B^*}, \quad (5)$$

which links the zero-field Drude resistivity with parameters (ρ^*, B^*) owned to point of flatness.

As expected, for zero slope $\gamma = 0$ one obtains $\rho_D^0 = \rho^*$ which would happens at infinite magnetic field. Using the experimental data for points of flatness $\rho^*(T), B^*(T)$ we calculate and, then plot in Fig.1,b the zero-field Drude resistivity $\rho_D^0(T)$. The later exhibits nearly linear behavior associated with carrier scattering on both the static defects and acoustic phonons. For stated[17] carrier density $n = 2.8 \cdot 10^{11}\text{cm}^{-2}$ we find and, then plot in Fig.4 the temperature dependent momentum mean free path of carriers. Remarkably, at $T = 1\text{K}$ we find the carrier mobility $1.4 \cdot 10^7\text{cm}^2\text{B/s}$ which exceeds by order of magnitude the estimation[17] made on the zero-field total re-

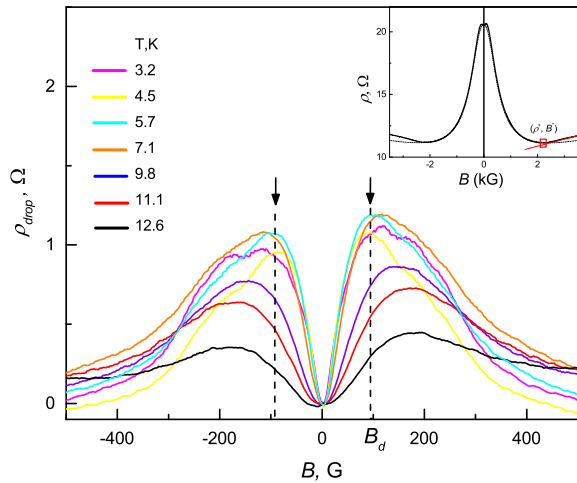


FIG. 3: The resistivity ρ_{drop} owned to droplets scattering given by difference(see inset) of experimental and calculated data depicted in Fig.1a and Fig.2a respectively for fixed temperature set denoted in the main panel.

sistivity $\sim 20\Omega$. We emphasize that our method provides accurate extraction of carrier mobility being hidden by harmful viscosity component.

Let us turn to the temperature dependence of the zero-field resistivity $\rho(T)$ followed Fig.1,a and, then plotted by magenta curve in Fig.1,b. Note that each data point on zero-field resistivity curve in Fig.1,b is given by Eq.(3) under condition $\xi = \xi_0$ and, moreover $\rho_D = \rho_D^0$. If so, for certain temperature one can solve primitive transcendental Eq.(3) and, then find the zero-field Gurzhi parameter ξ_0 for certain temperature. The result, namely the dependence $\xi_0(T)$, is plotted in Fig.1b,inset.

We now attempt to recover the experimental NMR data seen in Fig.1a at all. At finite magnetic field the Gurzhi parameter can be written as it follows

$$\xi = \xi_0 \sqrt{1 + \left(\frac{2w^2}{r_c l_p \xi_0^2} \right)^2}. \quad (6)$$

Using Eq.(3),(6), the dependencies $l_p(T), \xi_0(T)$ jointly with complete form $\rho_D = \rho_D^0 + \gamma B$ of Drude resistivity and, finally adding the equation $r_c[\mu\text{m}] = 0.88/B[\text{kG}]$ for cyclotron radius we are able to fit each curve in Fig.1a. Our best result is shown in Fig.2a. The inset to Fig.4 provide an example of the fit quality for certain NMR curve. The sole fitting parameter is the stream effective width w_{eff} which is plotted in Fig.2b. Apart from slight drop in temperature the effective width $w_{eff} \sim 9.6\mu\text{m}$ is found to be much less than nominal channel size $200\mu\text{m}$ [17]. While the temperature shift of the effective channel width remains puzzling its reduced size is well understood[16] in terms of artificial defects in form of Ga droplets. Usually, it was argued[9] that the average distance between

the droplets, d , may define the actual effective width of the stream. We now confirm this hypothesis analyzing two low-field peaks (\downarrow) seen, for example, in Fig.1a. We attribute these peaks to an extra diffusive scattering on droplets edges similar to that known[28] for Hall bar walls scattering. To make quantitative check, for fixed temperature we use NMR curve in Fig.1a and, then subtract the hydrodynamic component depicted in Fig.2a. We associate this resistivity $\rho_{drop}(B)$ with droplets and then plot it Fig.4 for certain temperatures. At low temperatures the peaks position $B_d = \pm 96\text{G}$ owned to scattering on droplets edges remains unchanged. We argue that the scattering would be suppressed when the associated cyclotron radius $r_c = 9.2\mu\text{m}$ becomes less than inter droplet distance d which, in turn, is comparable with effective stream width w_{eff} . Hence, we demonstrated that $w_{eff}, d \sim 9\mu\text{m}$. The rough estimation of the actual droplet density yields a value $(\pi d^2/4)^{-1} = 1.5 \cdot 10^5 \text{cm}^{-2}$ comparable with that $\sim 7.7 \cdot 10^4 \text{cm}^{-2}$ reported[16] for most disordered samples.

Taking into account the effective width one may readily find the electron-electron scattering length $l_{ee} = \frac{1}{l_p} \left(\frac{w_{eff}}{\xi_0} \right)^2$ plotted as a function of temperature in Fig.2b. We put on the same plot the result of Ref.[9] followed from Eq.(3) and, moreover, a priori assumptions on the carriers scattering rates. Apart from the mean free path l_p which is higher compared to that reported in Ref.[9], our analysis demonstrates completely different functional dependence of e-e scattering length l_{ee} on temperature. Being rather unexpected within Fermi liquid scenario[29], namely $l_{ee} \sim T^{-2}$, our finding awaits a further profound study.

Finally, we will check the consistency of our approach by analysis of the magnetic field B^* matched to certain point of flatness. The later can be evaluated as it follows

$$B^* = \left(\frac{e R_k}{2\alpha\gamma} \right)^{1/2} \cdot \frac{\sqrt{\xi_0}}{w_{eff}}. \quad (7)$$

where $R_k = h/e^2$ and $\alpha = 1/137$ are the Klitzing and fine-structure constant respectively. According to Eq.(7) the temperature dependence $B^*(T)$, if found experimentally, then could be used to recover Gurzhi parameter ξ_0 assuming a constant effective width. In present case we are, however, obliged to use both the temperature dependent variables $\xi_0(T), w_{eff}(T)$. The result of calculations by the red line in Fig.???. A perfect coincidence of experimental and calculated curves confirms applicability of our method.

In conclusion, we analyzed the rough NMR data using Gurzhi model adapted for two-dimensionless carriers. No special assumptions were made a priori on the electron-electron scattering rate. We suggest a method for accurate determination of the two-dimensional carrier mobility and, then obtain extraordinary coincidence of calculation results with respect to experimental data down to the lowest temperature $T = 0.25\text{K}$. Our method allows us to identify the intrinsic value of mobility be-

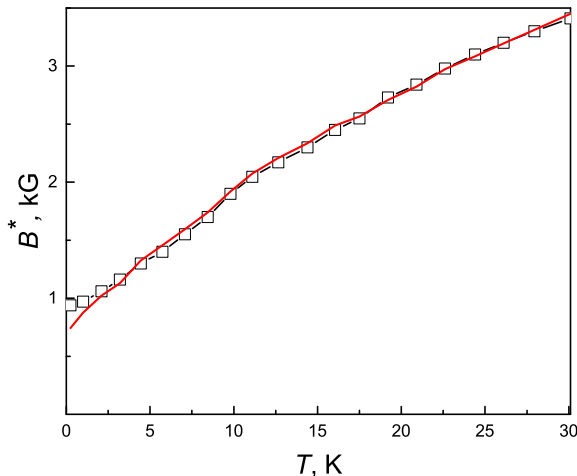


FIG. 4: Temperature dependence of the specific magnetic field B^* owned to points of flatness in Fig.1. Red line depicts the result of calculations according to Eq.(7).

ing higher than that obtained by conventional methods. We demonstrate unexpected temperature behavior of electron-electron mean free path and, hence carrier viscosity which could be a subject of further experimental and theoretical studies. We propose our method of NMR transport data analysis as a powerful tool regarding two-dimensional viscometry and mobility estimation.

Acknowledgments

The author thanks P. S. Alekseev and A. P. Dmitriev for useful discussions and M. A. Zudov for experimental data availability.

-
- [1] R.N. Gurzhi, Zh. Eksp. Teor. Fiz. **44**, 771 (1963) [Sov. Phys. JETP **17**, 521 (1963)].
 - [2] R.N. Gurzhi and S.I. Shevchenko, Sov. Phys. JETP **27**, 1019 (1968).
 - [3] R. N. Gurzhi, Sov. Phys. Uspekhi **11**, 255 (1968).
 - [4] S. Conti and G. Vignale, Phys. Rev. B **60**, 7966 (1999).
 - [5] I. Tokatly and O. Pankratov, Phys. Rev. B **60**, 15550 (1999).
 - [6] B. Bradlyn, M. Goldstein, and N. Read, Phys. Rev. B **86**, 245309 (2012).
 - [7] C. Hoyos and D. T. Son, Phys. Rev. Lett. **108**, 066805 (2012).
 - [8] A. Principi, G. Vignale, M. Carrega, and M. Polini, Phys. Rev. B **93**, 125410 (2016).
 - [9] P.S. Alekseev, Phys. Rev. Lett. **117**, 166601 (2016).
 - [10] L.W. Molenkamp and M.J.M. de Jong, Phys. Rev. B **49**, 5038 (1994).
 - [11] M.J.M. de Jong and L.W. Molenkamp, Phys. Rev. B **51**, 13389 (1995).
 - [12] Y. Dai, R. R. Du, L. N. Pfeiffer, and K. W. West, Phys. Rev. Lett. **105**, 246802 (2010).
 - [13] L. Bockhorn, P. Barthold, D. Schuh, W. Wegscheider, and R. J. Haug, Phys. Rev. B **83**, 113301 (2011).
 - [14] A.T. Hatke, M.A. Zudov, J. L. Reno, L. N. Pfeiffer, and K. W. West, Phys. Rev. B **85**, 081304(R) (2012).
 - [15] R.G. Mani, A. Kriisa, and W. Wegscheider, Sci. Rep. **3**, 2747 (2013).
 - [16] L. Bockhorn, I. V. Gornyi, D. Schuh, C. Reichl, W. Wegscheider, and R. J. Haug, Phys. Rev. B **90**, 165434 (2014).
 - [17] Q. Shi, P. D. Martin, Q. A. Ebner, M. A. Zudov, L. N. Pfeiffer, and K. W. West, Phys. Rev. B. **89**, 201301(R) (2014).
 - [18] A. T. Hatke, M. A. Zudov, L. N. Pfeiffer, and K. W. West, Phys. Rev. B **83**, 121301(R) (2011).
 - [19] Y. Dai, K. Stone, I. Knez, C. Zhang, R. R. Du, C. Yang, L. N. Pfeiffer, and K. W. West, Phys. Rev. B **84**, 241303(R) (2011).
 - [20] P.J.W. Moll, P. Kushwaha, N. Nandi, B. Schmidt, and A.P. Mackenzie, Science **351**, 1061 (2016).
 - [21] J. Gooth, F. Menges, C. Shekhar, V. Suess, N. Kumar, Y. Sun, U. Drechsler, R. Zierold, C. Felser, and B. Gotsmann, Nat. Commun. **9**, 4093 (2018).
 - [22] G.M. Gusev, A.D. Levin, E.V. Levinson, and A.K. Bakarov, Phys. Rev. B **98**, 161303 (2018).
 - [23] G.M. Gusev, A.D. Levin, E.V. Levinson, and A.K. Bakarov, AIP Advances **8**, 025318 (2018).
 - [24] A. D. Levin, G. M. Gusev, E. V. Levinson, Z. D. Kvon, and A. K. Bakarov, Phys. Rev. B **97**, 245308 (2018)
 - [25] B. Horn-Cosfeld, J. Schluck, J. Lammert, M. Cerchez, T. Heinzl, K. Pierz, H. W. Schumacher, and D. Mailly, Phys. Rev. B **104**, 045306 (2021).
 - [26] X. Wang, P. Jia, Rui-Rui Du, L.N. Pfeiffer, K.W. Baldwin, and K.W. West, Phys. Rev. B **106**, L241302 (2022).
 - [27] S. Chapman and T. G. Cowling, The Mathematical Theory of Non-Uniform Gases (Cambridge University, Cambridge, 1970) 3rd edition, Ch. 19 [(Cambridge University, Cambridge, 1953) 2nd edition, Ch. 18].
 - [28] T.J. Thornton, M.L. Roukes, A. Scherer, and B. P. Van de Gaag, Phys. Rev. Lett. **63**, 2128 (1989).
 - [29] I.Ia. Pomeranchuk, J. Exp. Theor. Phys. **20**, 919 (1950).